NCREE NEWSLETTER

December 2015 VOL. 10 NO. 4



CONTENTS

- Effect of Vertical Excitation on Horizontal Performance of Rolling-type Isolation Bearings
- Response Shaping of Sloped Rolling-type Isolation Devices using Embedded Electromagnets
- An Optimal Design Formula for Viscous Damping Ratio in an Isolation System with Consideration of Site Classification
- Performance of Three On-site Earthquake Early Warning Techniques in Taiwan
- Seismic Evaluation and Strengthening Guidelines for Hospital Buildings and Associated Simplified Evaluation Program for Equipment
- Current Status of NCREE Southern Laboratory
- Introduction and Demonstrating Earthquake Engineering Research in Schools (IDEERS) 2015
- The International Training Program for Seismic Design of Structures 2015
- International Workshop on Advanced Earthquake Engineering Testing and Simulation for Near-Fault Ground Motions and Multiple Hazard Load Effects

DIRECTOR

Kuo-Chun Chang

EDITORS

Wang-Chuen Lin

Cho-Yen Yang

National Center for Research on Earthquake Engineering

Effect of Vertical Excitation on Horizontal Performance of Rolling-type Isolation Bearings

Wang-Chuen Lin, Assistant Researcher, Shiang-Jung Wang, Research Fellow, NCREE

As shown in Figure 1, the sloped rolling-type isolation bearings were composed of three bearing plates (hereinafter denoted as upper, intermediate, and lower bearing plates) and cylindrical rollers. This study aims to derive generalized equations of motion for a sloped rolling-type isolation bearing in which the rollers move between two arbitrary sloping surfaces. The influences arising from the neglect of higher order terms of sloping angles and vertical excitations on the transmitted horizontal acceleration responses of the bearing are numerically discussed.

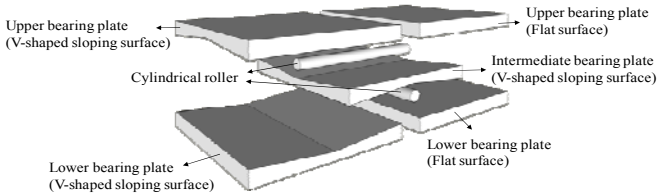
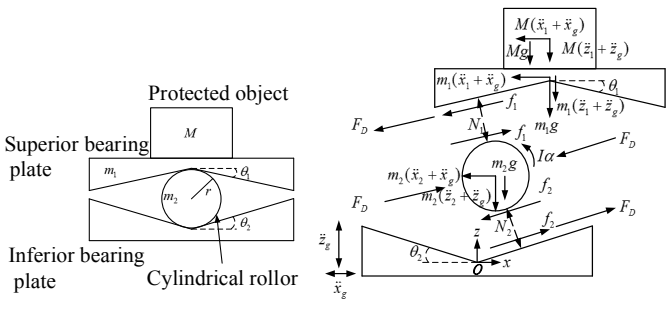


Fig. 1. Schematic drawings of sloped rolling-type isolation bearings

A simplified model comprising a roller sandwiched between two V-shaped surfaces was designed with different sloping angles θ_1 and θ_2 to represent the dynamic behavior of an isolation bearing in one principle horizontal direction and in the vertical direction in Figure 2(a). M, m_1, and m_2 represent the seismic reactive masses of the protected object, superior bearing plate, and roller, respectively and r denotes the radius of the roller. The free body diagrams when $\mathrm{sgn}(x_1)=\mathrm{sgn}(x_2)=1$ and $\mathrm{sgn}(\dot{x}_1)=\mathrm{sgn}(\dot{x}_2)=1$ are shown in Figure 2(b), in which $x_1(z_1)$, $\dot{x}_1(\dot{z}_1)$, and $\ddot{x}_1(\ddot{z}_1)$ are the horizontal (vertical) displacement, velocity, and acceleration responses of the protected object and superior bearing plate relative to the origin O, respectively; $x_2(z_2)$, $\dot{x}_2(\dot{z}_2)$, and $\ddot{x}_2(\ddot{z}_2)$ are the horizontal (vertical) displacement, velocity, and acceleration responses of the roller relative to the origin O, respectively; I is the moment of inertia of the roller; α is the angular acceleration of the roller; $f_1(f_2)$ and $N_1(N_2)$ are the rolling friction force and normal force acting between the superior bearing plate and roller (between the roller and inferior bearing plate), respectively; and F_D is the built-in friction damping force acting parallel to the slope of the bearing plates.



(a) Static condition (b) Free body diagrams

Fig. 2. Simplified models used in this study

By considering the dynamic force and moment equilibrium shown in Figure 2(b), a total of nine variables named the exact generalized solutions can be solved. The horizontal acceleration response $\ddot{x}_1$ is given in Equation (1).

$$\ddot{x}_1=\frac{-(\cos\theta_1+\cos\theta_2)}{2(M+m_1)[1+\cos(\theta_1-\theta_2)]}\{2F_D\,\mathrm{sgn}(\dot{x}_1)+(M+m_1)[\ddot{x}_g(\cos\theta_1+\cos\theta_2)+(g+\ddot{z}_g)(\sin\theta_1+\sin\theta_2)\mathrm{sgn}(x_1)]\} \quad (1)$$

Two assumptions are made: (1) $\cos^2\theta_1\approx 1$, $\sin^2\theta_1\approx 0$, and $\sin\theta_1\sin\theta_2\approx 0$; and (2) the term involving $\ddot{z}_g$ is neglected. The nine variables can be obtained and named the simplified generalized solutions. The simplified form of Equation (1) is denoted as Equation (2):

$$\ddot{x}_1=\frac{-(\cos\theta_1+\cos\theta_2)}{4(M+m_1)}[2F_D\,\mathrm{sgn}(\dot{x}_1)+(M+m_1)g(\sin\theta_1+\sin\theta_2)\mathrm{sgn}(x_1)]-\ddot{x}_g \quad (2)$$

A simplified model composed of a roller with a radius of 100 mm is employed as shown in Figure 2(a). A total of 25 cases of bearings which used a combination of θ_1 and θ_2 varying from 2° to 6° with an increment of 1° is designed and numerically studied. The built-in friction damping forces are designed to be the same for the 25 cases and are equal to 301 N. The total seismic reactive mass, $M+m_1$, is designed to be 1000 N-sec^2/m. Considering the pounding prevention mechanism, an arc rolling range of 21.6 mm in the horizontal direction is designed at the intersection of the two inclines of the V-shaped surfaces. As detailed in Table 1, three recorded earthquake histories and three generated acceleration histories are adopted.

Table 1. Acceleration input program

Acc. input	Input information or response spectrum condition	Excitation direction		Different input PA scales (g) 25%	50%	75%	100%
El Centro	IMPVALL/I-ELC180 IMPVALL/I-ELC-UP Imperial Valley, U.S., 1940/05/19	Unilateral	X	0.08	0.16	0.23	0.31
		Biaxial	X	0.08	0.16	0.23	0.31
			Z	0.05	0.11	0.16	0.21
Kobe	KOBE/KJM000 KOBE/KJM-UP Kobe, Japan, 1995/01/16	Unilateral	X	0.21	0.41	0.62	0.82
		Biaxial	X	0.21	0.41	0.62	0.82
			Z	0.09	0.17	0.26	0.34
ChiChi	CHICHI/CHY028-N CHICHI/CHY028-V Chi-Chi, Taiwan, 1999/09/21	Unilateral	X	0.19	0.38	0.57	0.76
		Biaxial	X	0.19	0.38	0.57	0.76
			Z	0.09	0.17	0.26	0.34
AC 156-1	RRS specified in AC156 Isolated equipment is placed at 3rd floor (8.75m in elevation) of a 7-story building (24m in height) at Taipei City	Unilateral	X	0.13	0.25	0.38	0.50
		Biaxial	X	0.13	0.25	0.38	0.50
			Z	0.06	0.13	0.19	0.25
AC 156-2	RRS specified in AC156 Isolated equipment is placed at 3rd floor (8m in elevation) of a 3-story building (12m in height) at Nantou County	Unilateral	X	0.25	0.50	0.75	1.00
		Biaxial	X	0.25	0.50	0.75	1.00
			Z	0.13	0.25	0.38	0.50

IEEE	RRS specified in IEEE Std 693TM-2005 for high performance level	Unilateral	X	0.25	0.50	0.75	1.00
		Biaxial	X	0.25	0.50	0.75	1.00
			Z	0.20	0.40	0.60	0.80

To separately and clearly discuss the extent of the influences arising from neglecting of higher order terms and vertical acceleration excitations on the horizontal acceleration predictions, two indices, ER_1 and ER_2, are defined as follows:

$$ER_1 = \frac{\max(|A_{UE}|) - \max(|A_{US}|)}{\max(|A_{US}|)} \times 100\% \quad (3)$$

$$ER_2 = \frac{\max(|A_{BE}|) - \max(|A_{UE}|)}{\max(|A_{UE}|)} \times 100\% \quad (4)$$

where A_{UE} and A_{BE} denote the horizontal acceleration predicted by Equation (1) under unilateral and biaxial excitations, respectively; and A_{US} represents the horizontal acceleration predicted by Equation (2) under unilateral excitations.

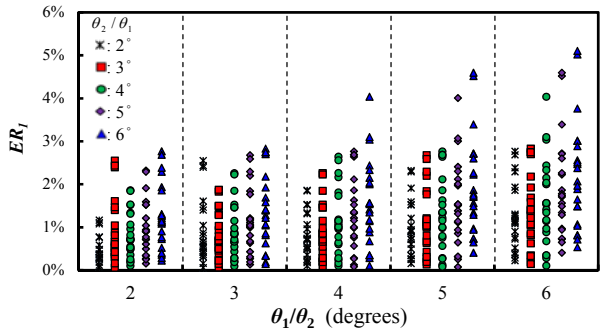


Fig. 3.Variations of ER_1 values under all unilateral acceleration inputs

It is found from Figure 3 that the larger the design sloping angle is, the more apparent effect revealed from neglect of higher order terms of sloping angles on the ER_1 value exerts. Nevertheless, in this study, the maximum ER_1 value is only 5.10% for the design case of (θ_1, θ_2)=(6°,6°) under unilateral-100%-ChiChi. Therefore, it can be concluded that the effect of higher order terms of sloping angles on the acceleration prediction accuracy is very limited and can be rationally negligible in engineering practice.

It can be found in Figure 4 that the differences between the maximum horizontal acceleration predictions by using the exact generalized solutions under unilateral and biaxial excitations, i.e. the ER_2 value, might be worthy of attention. It is apparent that a larger vertical peak acceleration (PA) value will lead to a more significant effect without regard to vertical acceleration excitations on the ER_2 value. As shown in Figure 5, it is evident that in the same design case, the larger the vertical PA value is, the more significant effect without considering vertical acceleration excitations on the ER_2 value produces. In this study, the maximum ER_2 value is 36.59% in the design case of (θ_1, θ_2)=(2°,2°) under biaxial-100% -IEEE, which might not be very acceptable compared to the maximum ER_1 value mentioned, i.e. 5.10%. Therefore, to preclude a non-conservative design result, the effect of vertical acceleration excitations on the maximum transmitted horizontal acceleration response of the isolation bearing should be taken into account, especially when the vertical excitation possesses a larger PA value

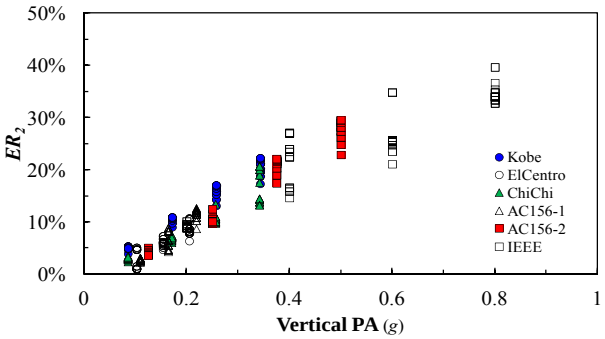


Fig. 4. Variations of ER_2 values under all biaxial acceleration inputs

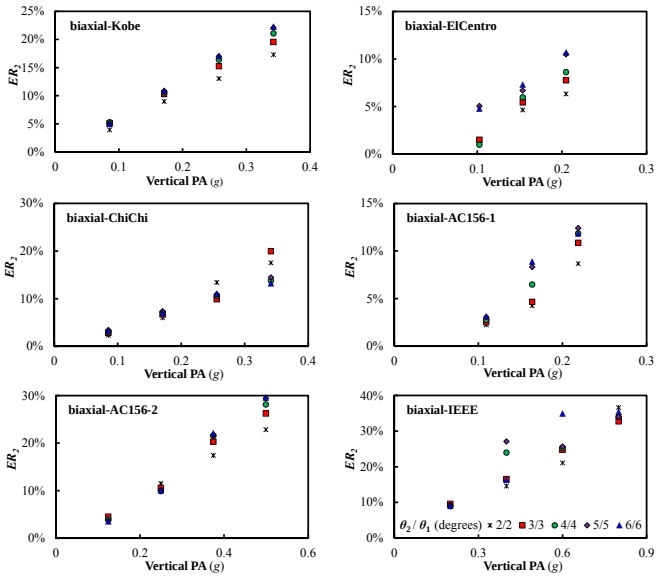


Fig. 5. Variations of ER_2 values with various vertical PA scales for five design cases of $\theta_1 = \theta_2$ under all biaxial acceleration inputs

To obtain a more comprehensive performance design procedure for the sloped rolling-type isolation bearing in which the cylindrical rollers move between two V-shaped surfaces designed with arbitrary sloping angles, an analytical model that considers more generalized equations of motion is developed in this study. A series of numerical studies are performed to quantitatively discuss the influences arising from neglecting of higher order terms and vertical excitations on the transmitted horizontal acceleration responses of the isolation bearing. The numerical results reveal that the effect of vertical acceleration excitations plays a crucial role in prediction accuracy compared to that of higher order terms of sloping angles. When the acceleration excitation possesses a considerable vertical component, adopting the exact generalized equations of motion rather than the simplified ones can achieve more precise and conservative analysis results for the sloped rolling-type isolation bearing.

Response Shaping of Sloped Rolling-type Isolation Devices using Embedded Electromagnets

Pei-Ching Chen, Associate Researcher, Shiang-Jung Wang, Research Fellow, NCREE

Sloped rolling-type isolation devices incorporating a built-in damping and pounding preventer possess the advantage of suppressing excessive displacement responses during severe excitations. However, the control performance is restricted as passive control devices are not capable of effectively coping with the variation of earthquakes. In this study, a novel controllable damping module that embeds elastic springs and electromagnets is proposed to control the sliding friction of the rolling-type isolation device. By varying the input currents to the electromagnets, the corresponding magnetic forces can be used to control the normal force, leading to indirect semi-active control of the sliding friction force, which can purposely shape the hysteresis response of the existing isolation device.

The controllable damping module is composed of four electromagnets, two elastic springs, one bearing plate, and one cover plate as shown in Figure 1. The cover plate is intended to apply a preloading force to the elastic springs as well as the contact force between the electromagnets and the steel plate installed inside the cover plate. The bearing plate is used to embed the electromagnets and elastic springs. When installing the module, the cover plate pushes the elastic springs until the steel plate contacts the electromagnets. Then the cover plate and bearing plate are connected tightly by screws so that the preloading force can be determined by the elastic modulus of the spring and the difference in height between the spring and the electromagnet. Finally, the controllable damping module is connected to the base isolation system by two rods inserted into the rollers. This mechanism can make a synchronous movement between the rollers and the damping module. Meanwhile, the rubber is also connected to the base isolation system so that a friction force can be generated between the rubber and the steel plate when relative motion of the two parts occurs.

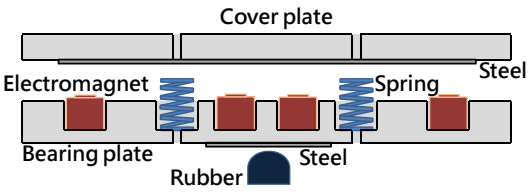


Fig. 1. Components of the damping module

Validation tests were performed by using a uni-axial shaking table to conceptually verify the feasibility and effectiveness of the proposed controllable damping module. The dSPACE hardware was adopted to collect the measured signal and calculate the control voltage for the electromagnets. In addition, a voltage control current source (VCCS) was used to translate the calculated control voltage to control current. In the experimental validation, the VCCS was aimed at supplying a control current to the electromagnets, which was linearly related to the calculated control voltage from the dSPACE by a calibration constant.

Four simple control algorithms were adopted to validate the effectiveness of the proposed damping module in terms of hysteretic loop shaping including (a) maximum damping case in which the electromagnets were turned off leading to the maximum generated friction force; (b) magnet-on case in which the maximum allowable current served as an input to the electromagnets; (c) control-1 case in which the electromagnets were turned on when the isolation device was moving away from the original position and turned off when the device was moving toward the original position; and (d) control-2 case which was operated in reverse to control-1. Note that both the maximum damping and magnet-on cases can be treated as passive devices since the friction force remained invariant.

A continuous sinusoidal input with a frequency of 1 Hz and a peak ground acceleration of 200 gal was adopted for simplicity of testing. The sampling rate of each test was 200 Hz. Figure 2 shows the experimental results. The maximum damping case was able to dissipate much more energy compared with the undamped case. In the magnet-on case, an inferior energy dissipation capability can be observed compared with the maximum damping case. In the control-1 case, the transmitted acceleration was identical to the magnet-on case when the upper plate moved away from the original position. The transmitted acceleration then switched to the value close to the maximum damping case. A similar observation can be seen in the control-2 case.

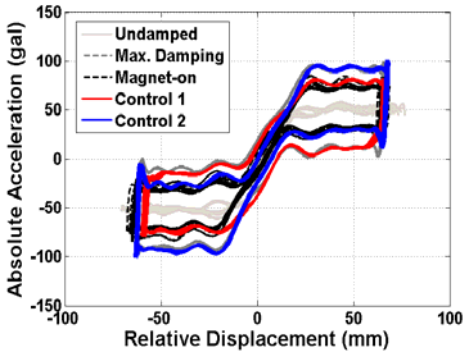


Fig. 2. Experimental results of the response shaping

Conclusively, the experimental results demonstrate that the control mechanism of the controllable damping module developed in this study is feasible and effective as expected. It also provides base isolator devices with additional flexibility and controllability, and prevents protected objects from severe damage in a modern and high-tech approach.

An Optimal Design Formula for Viscous Damping Ratio in an Isolation System with Consideration of Site Classification

Cho-Yen Yang, Assistant Researcher, Lap-Loi Chungn, Research Fellow, NCREE
Yang-Chih Fan, Bao-Jyun Lu, National Taiwan University

In an isolation system with viscous damping, there are two important factors, namely isolation frequency and damping ratio. The absolute acceleration of a superstructure increases regardless of whether the damping ratio increases or decreases. Thus, an optimal damping ratio that minimizes the absolute acceleration of superstructure exists. One research study proposed an optimal design formula where white noise excitation was taken into consideration. However, that design formula may not be feasible in Taiwan. Therefore, a design formula by a new approach considering site classification is proposed.

From the seismic design code in Taiwan, a design force is determined by considering the property of a site. Thus, the seismic records from four types of sites including type 1, 2, 3, and the Taipei basin around Taiwan are selected to be the excitation inputs for the regression of the proposed optimal design formula. The superstructure with or without structural damping ratio is simplified to a single degree-of-freedom system. To simplify the derivation of the optimal design formula, two parameters including mass ratio defined as mass of a superstructure divided by the total mass of the entire structural system and frequency ratio defined as structural frequency divided by isolation frequency are adopted. In addition, the optimal damping ratio is defined as the corresponding damping ratio that minimizes the acceleration ratio which is defined as the root mean square of structural absolute acceleration with isolation divided by the one without isolation. The optimal design formula is started from the case of the superstructure without structural damping and is sequentially regressed by varying the isolation frequency, the mass ratio, and the frequency ratio. Furthermore, the design formula of the structural isolation with structural damping can be obtained by extending the regression of varying structural damping ratio.

Due to the consideration of site property to the design formula, a total of 177 seismic records measured from the four sites around Taiwan are considered to be input excitations for optimization and regression. An isolation frequency within 0.2 to 0.5 Hz, a frequency ratio within 2 to 10, and a mass ratio within 0.5 to 0.9 are considered. For the design formula of structural isolation with structural damping, a structural damping ratio within 0 to 0.05 is considered. From the regression results, the design formulas for site types 1, 2, and 3 are similar; thus, the optimal design formula is classified into two major types, which are the Taipei basin and the non-Taipei basin.

Non-Taipei basin (without structural damping):

$$\begin{aligned}\zeta_{\mathrm{i,opt,undamped}} = & \left\{\left(-0.0597+1.1512R_{\mathrm{m}}-1.0438R_{\mathrm{m}}^{2}\right)+\left(0.0817-0.4724R_{\mathrm{m}}+0.3716R_{\mathrm{m}}^{2}\right)R_{\mathrm{f}}\right. \\ & \left.+\left(-0.0065+0.0306R_{\mathrm{m}}-0.0225R_{\mathrm{m}}^{2}\right)R_{\mathrm{f}}^{2}\right\} \\ & +\left\{\left(1.016-2.6924R_{\mathrm{m}}+2.9214R_{\mathrm{m}}^{2}\right)+\left(-0.1668+0.7473R_{\mathrm{m}}-0.5881R_{\mathrm{m}}^{2}\right)R_{\mathrm{f}}\right\}f_{\mathrm{i}} \\ & +\left\{\left(-1.615+4.441R_{\mathrm{m}}-3.9008R_{\mathrm{m}}^{2}\right)+\left(0.3051-0.9813R_{\mathrm{m}}+0.6974R_{\mathrm{m}}^{2}\right)R_{\mathrm{f}}\right\}f_{\mathrm{i}}^{2}\end{aligned}$$

Taipei basin (without structural damping):

$$\begin{aligned}\zeta_{\mathrm{i,opt,undamped}} = & \left\{\left(0.4327-0.5894R_{\mathrm{m}}\right)-\left(0.1493-0.1465R_{\mathrm{m}}\right)R_{\mathrm{f}}+\left(0.0091-0.0086R_{\mathrm{m}}\right)R_{\mathrm{f}}^{2}\right\} \\ & +\left\{\left(-0.7806+2.7737R_{\mathrm{m}}\right)+\left(0.4932-0.4788R_{\mathrm{m}}\right)R_{\mathrm{f}}-\left(0.0249-0.0225R_{\mathrm{m}}\right)R_{\mathrm{f}}^{2}\right\}f_{\mathrm{i}} \\ & +\left\{\left(0.5924-1.978R_{\mathrm{m}}\right)-\left(0.0861-0.164R_{\mathrm{m}}\right)R_{\mathrm{f}}\right\}f_{\mathrm{i}}^{2}\end{aligned}$$

The two equations above represent the optimal design formulas for the cases of structural isolation without structural damping in the Non-Taipei basin and the Taipei basin sites. Similarly, the optimal design formulas for the cases of structural isolation with structural damping can be obtained by regressing one more step of the relationship between the optimal damping ratio and the structural damping ratio. The results are given as follows:

Non-Taipei basin (with structural damping):

$$\zeta_{\mathrm{i,opt,damped}}/\zeta_{\mathrm{i,opt,undamped}}=1+0.5066\zeta_{\mathrm{s}}+9.188\zeta_{\mathrm{s}}^{2}$$

Taipei basin (with structural damping):

$$\zeta_{\mathrm{i,opt,damped}}/\zeta_{\mathrm{i,opt,undamped}}=1-0.0476\zeta_{\mathrm{s}}+6.487\zeta_{\mathrm{s}}^{2}$$

For the case of structural isolation without structural damping, the optimal damping ratio can be calculated by substituting isolation frequency, frequency ratio, and mass ratio into the formulas, and for the case of structural isolation with structural damping, just one more parameter, namely structural damping ratio, is additionally required. Thus, it is easy to implement since only a maximum of four parameters are required for the proposed optimal design formulas to calculate the optimal damping ratio. The proposed design formulas have also been verified through numerical simulations in a real application to ensure that the structural isolation system is effective and no failure occurs due to excessive isolation displacement. Consequently, the proposed optimal design formulas might be valuable and feasible for reference in practical applications.

From the proposed optimal design formula above, engineers can substitute those parameters into the equations that can be obtained from conventional structural design procedures. Based on the optimal damping ratio calculated from the formulas, engineers can tune the damping ratio by some other construction considerations.

Performance of Three On-site Earthquake Early Warning Techniques in Taiwan

Ting-Yu Hsu, Research Fellow, Shieh-Kung Huang, Hung-Wei Chiang, Assistant Researcher, NCREE
Pei-Yang Lin, Research Fellow, Kung-Chun Lu, Assistant Researcher, NCREE
Kuo-Liang Wen, Division Director, Yun-Ju Lai, Research Assistant, NCREE

Taiwan suffers from destructive seismic hazards due to in-land earthquakes. Therefore, regional earthquake early warning (EEW) systems are not suitable for Taiwan as the lead-time before a destructive earthquake wave arrives that is given by a regional EEW system can be null. On the other hand, an on-site EEW system can provide more lead-time at a region close to an epicenter since only the seismic information for the target site is required. Recently, a new support vector regression (SVM) method has been developed. However, until now, the most popular on-site algorithms in Taiwan have been the TauC-Pd-Attenuation (TPA) method and the Pd-Threshold method (PdT). This study aims to evaluate the performance of these three methods using 89,433 earthquake data of the Taiwan Strong Motion Instrumentation Program (TSMIP) and the 1,191 earthquake data of EEW stations at schools established by the National Center for Research on Earthquake Engineering (NCREE) in Taiwan.

The three on-site EEW methods are summarized below:

1. TauC-Pd-Attenuation Method (Tsai et al., 2009)

The TPA method is mainly based on three regression models. Firstly, TauC and Pd are calculated from the first three seconds of the vertical ground acceleration after the arrival of the P-wave. Then, the earthquake magnitude (M) and hypocenter distance (R) can be estimated. Finally, the PGA is estimated according to the PGA attenuation law in Taiwan.

2. Pd-Threshold method (Wu and Kanamori, 2005b)

This method considers an earthquake with a Pd value larger than 0.5 cm as a destructive earthquake, and then an alert is issued. This method has been embedded into the P-Alert low cost sensor.

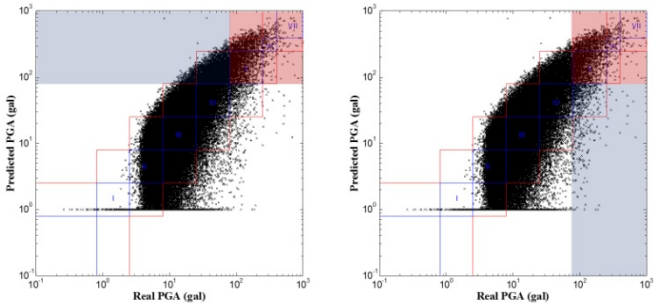
3. Support Vector Regression Method (Hsu et al., 2013)

This method predicts the PGA using six P-wave features from the first three seconds of the vertical ground acceleration after the arrival of the P-wave using a SVM model.

Referring to the Japan Meteorological Agency (JMA), this study considered only the measured earthquakes and predicted earthquakes with intensities equal to or greater than 4 when calculating the prediction accuracy. If the difference between the estimated and measured intensity was less than or equal to 1, the prediction was treated as an accurate one. The Prediction Accuracy Rate (PAR) is defined as the number of accurate predictions divided by the number of trigger events. It was used as a basic estimation index for both the TPA method and the SVM method since PGA was not predicted by the PdT method.

We considered that an earthquake with intensity $\geqq 5$ should trigger an alarm since it may cause damage. The False Alarm Ratio (FAR) and the Missed Alarm Ratio (MAR) are used to check the reliability of issued alarms of the EEW methods. An issued alarm where the measured seismic intensity<5 is defined as a false alarm. If the measured seismic intensity$\geqq 5$ but an alarm is not issued, then it is defined as a missed alarm. Therefore, the FAR (%) is the ratio of the number of issued alarms with seismic intensity<5 and the total number of issued alarms. Meanwhile, the MAR (%) is the ratio of the number of events with measured seismic intensity$\geqq 5$ without an alarm and the number of all seismic events with measured seismic intensity$\geqq 5$.

Finally, in order to compare the three aforementioned methods, the Pd threshold value of the PdT method was reduced to 0.025 cm so that the MAR values of the three methods were similar. The PAR, FAR, and MAR of the three methods using the TSMIP data and the NCREE on-site station data are summarized in Table 1. The results show that the SVM method can provide the least rate of false positive alarms under the assumed condition. In other words, the SVM method can provide the most reliable and accurate earthquake early warnings among these three methods if we consider that earthquakes with intensity$\geqq 5$ should be alarmed.



(a) (b)

Fig. 1. The measured PGA and the predicted PGA of the 89,433 TSMIP data using the SVM method

Table 1. The accuracy of the SVM, TPA and PdT methods

Database	TSMIP			NCREE on-site stations at schools		
Method	PAR(%)	FAR(%)	MAR(%)	PAR(%)	FAR(%)	MAR(%)
SVM	91.04	65.26	19.42	77.94	80.00	0.00
TPA	67.51	80.37	19.19	39.86	91.67	25.00
PdT (0.025cm)	-	85.02	18.06	-	93.86	0.00

Seismic Evaluation and Strengthening Guidelines for Hospital Buildings and Associated Simplified Evaluation Program for Equipment

Juin-Fu Chai, Research Fellow, NCREE,
Fan-Ru Lin, Assistant Researcher, NCREE; Tzu-Chieh Chien, Research Assistant, NCREE

The most important issue for a designated responsibility hospital for acute services is to maintain its emergency medical functions continuously. However, during recent earthquakes, not only hospital building structures but also medical equipment inside were seriously damaged, which resulted in a significantly limited emergency medical capacity of hospitals. This implies that the earthquake-resistance capacity of hospitals for emergency treatment should be upgraded to remain functional with regard to their engineering structures, medical facilities, electricity and water supply, and information services after major earthquakes.

Currently, most of the Ministry of Health and Welfare hospitals in Taiwan have completed simplified evaluations of the seismic capacity of their building structures. However, due to a lack of information about evaluation methods for nonstructural components and systems (NSCS), the electrical and mechanical systems were only roughly visually inspected, and the seismic capacity of the medical equipment and piping systems has still not been considered. Therefore, "Seismic Evaluation and Strengthening Guidelines for Hospital Buildings" is presented by the NCREE as the achievement of a three-year National Science Council project. As proposed, this guideline consists of three major parts: (1) An upgrading strategy for the seismic performance of hospitals, including the classification of building structures and NSCS of hospitals, and associated seismic rehabilitation objectives; (2) Seismic evaluation and strengthening guidelines for hospital building structures; and (3) Seismic evaluation and strengthening guidelines for NSCS in hospitals.

The hospital rehabilitation objective is defined to meet specified rehabilitation goals. Each goal shall consist of a target performance level and an earthquake hazard level. From strict to lenient, the structural target performance level for a hospital shall be selected from three discrete performance levels, namely SPL-A, SPL-B, and SPL-C. Per SB1953, the NSCS target performance level shall be selected from five levels labeled NPL1 to NPL5; the statements are shown in Table 1 and Table 2.

Owing to the onerous work required to improve the seismic performance of various NSCS, a simplified program is established using Microsoft Excel software to execute a preliminary seismic evaluation and retrofit design for individual pieces of medical equipment. Users are asked to fill in blanks with hospital information and the parameters of selected equipment. The program then identifies the performance objective of each piece of equipment. It also determines whether the equipment should be retrofitted or not. In addition, preliminary designs of post-installation anchor bolts for seismic retrofitting against specified seismic demands can be checked automatically by the program. The user interface of the program is shown in Figure 1. More studies are underway, including on the development of a seismic evaluation and design program for equipment attached to a wall or ceiling, and for those strengthened by z-shape stoppers or welding.

Table 1. Structure target performance level (I=1.0 or I=1.5)

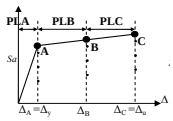
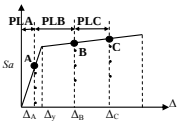
Earthquake Level	Target performance level	I = 1.0	I = 1.5
EQL-1	PLA		
EQL-2	PLB		
EQL-3	PLC		

Table 2. Hospital rehabilitation goals ('general' designated responsibility hospitals)

Earth-quake Level	Object		Rehabilitation Goals
EQL-1	Structures	PLA	Keep the same as prior to earthquake
	NSCS	NPL4	Immediate Occupancy for human occupied areas
EQL-2	Structures	PLB	Return to the original after repair in short time
	NSCS	NPL3	Immediate Occupancy for essential care areas
EQL-3	Structures	PLC	Prevent Collapse to ensure people exit safely
	NSCS	NPL2	Life Safety

*EQL-1: Frequently occurring small earthquake
*EQL-2: Designed earthquake level with a return period of 475 years
*EQL-3: Maximum considered earthquake level with a hazard of 2500 years

Number and Name			
Number:		Normal Supply System-	Normal Supply System-
Name:		Water Chiller Unit	Water Chiller Unit
Clasification			
Types:	MENU	Mechanical Equipment	Mechanical Equipment
Sorts:	MENU	HVAC System Component	HVAC System Component
Categories:	MENU	Vibration isolated	Vibration isolated
Location			
Location:	MENU	Others Human Occupied	Essential Care Areas
Floor:	Number (R for Roof,-1~-5 for Basement)	R	R
Parameter			
Weight (W_p) :	kgf	2000	750
Supporting Structural Component	MENU	Floor	Floor
Dimension:	Length of X-Axies (L_p) m	2.26	2.20
	Length of Y-Axies (L_Y) m	2.15	0.66
	Height (Containes Included) (h_i) m	2.40	1.96
Eccentric			
X-Axis Eccentric :	(Filled with Y or N)	Y	N
X-Axis Distance between the Edge to the Center of Gravity :	(Blank Space for Non-Eccentric or Uncertain) (L_{ex})	1.00	
Y-Axis Eccentric :	(Filled with Y or N)	Y	N
Y-Axis Distance between the Edge to the Center of Gravity :	(Blank Space for Non-Eccentric or Uncertain) (L_{ey})	1.00	
Z-Axis Eccentric :	(Filled with Y or N)	N	N
Z-Axis Distance between the Edge to the Center of Gravity :	(Blank Space for Non-Eccentric or Uncertain) (h_{ez})		
Surrounding			
Connection with Structure :	MENU	Non-Fixed	Non-Fixed
Material of Floor Surface :	MENU	Rubber	Rubber
Material of floor :	MENU	Concrete	Plastic flooring
Lean on the Wall :	MENU	Independent	Independent
Seismic Evaluation Required		Y	Y
Performance Level		NPL4	NPL3
Earthquake Hazard Level		DBE	MCE
Seismic Response of Equipment		Sliding	Sliding
Necessary for Strengthening		Y	Y
Bolt Strenthening	(Blank Space for No Necessary Strenthen)		
Number of bolts on X-Axies :		4	2
Number of bolts on Y-Axies:		4	2
Type or Size:	MENU	Hilti-M10	Hilti-M10
Depth in concrete:	in	4.00	3.00
Anchorage on Concrete or Other Material :	MENU		
Strength of Base Material :	psi	2800	2800
Result		OK	NO!!

Fig.1. The user interface of Evaluation Programs for Equipment

Current Status of NCREE Southern Laboratory

Fu-Pei Hsiao, Pei-Ching Chen, Associate Researcher, NCREE

A large number of active faults are located in Taiwan; therefore, the near-fault effect on structures has become an important issue for earthquake engineering studies. The safety of people living in the areas close to faults has been severely threatened. It is known that near-fault ground motions often contain a long period high velocity pulse in the fault-normal direction and permanent ground displacement. Generally, the spike in velocity may exceed 1500 mm/s, which is too large to be reproduced using the existing shaking table of NCREE. As a result, the National Applied Research Laboratories have planned to establish a second laboratory of NCREE in which a high performance 8 m × 8 m six degree-of-freedom seismic simulation testing system will be available to simulate the near-fault ground motions.

The second laboratory of NCREE is located at the eastern part of the Gueiren Campus of National Cheng Kung University in Tainan City. It is composed of a research building and a laboratory building. The research building is a three-story reinforced-concrete building with one-story basement. The construction work of the NCREE Southern Laboratory has been processed as a turnkey project. Formosa Builders, Inc. has become the contractor of the turnkey project assisted by Sinotech Engineering Consultants, Ltd. with professional construction management and construction supervision. The construction work has been ongoing since commencement from July 2015. The current construction work has proceeded to the structure of the first floor of the research building as well as the structure of the basement and the first floor of the laboratory building as shown in Figure 1. The construction of the research and the laboratory buildings will be completed by the end of April 2016 and July 2016, respectively. All the construction work of the NCREE Southern Laboratory will be accomplished and the Building Use permit will be obtained in October 2016.

The NCREE Southern Laboratory will be equipped with a high performance 6-DOF seismic shaking table test system, which can reproduce near-fault ground motions recorded, as well as a reaction wall and a strong floor test system, which can conduct component and structure testing. In addition to the two systems, a dynamic biaxial testing system (BATS), which is compatible with the functionality and capability of the existing MATS, will be established; its capacity and dynamic performance will be greatly enhanced. MTS Systems Corporation has become the facility supplier after winning the bid and signing the contract with NCREE in March, 2015. The design details of the high performance shaking table and BATS were reviewed carefully and thoroughly by NCREE in July and August, respectively. Currently, all the pipes and components are being manufactured. The tour for factory inspection has been arranged and the researchers and technicians in charge of operating the facilities will visit MTS and receive training in early March, 2016.

In order to get involved in the joint work of establishing the NCREE Southern Laboratory, NCREE has convened a research group to perform finite element analyses on the BATS, shaking table, reaction wall and strong floor, floating foundation, and the foundation piles and structures. In addition, a system identification of the air springs and viscous dampers that will be installed on the floating foundation are also being conducted to realize the dynamic characteristics of the seismic shaking table. The research results can provide the researchers in the future with a clear and overall understanding of the performance capacity and limitations of the new facilities.

After the new laboratory is completed, NCREE can provide better seismic experimental services to government agencies, academia, and industry, which are beneficial to improving public safety during earthquake disasters.



Fig.1. Current construction work of the NCREE Southern Laboratory

Introduction and Demonstrating Earthquake Engineering Research in Schools (IDEERS) 2015

Mu-Hsuan Li, Associate Technologist, NCREE

The fifteenth annual Introducing and Demonstrating Earthquake Engineering to Students (IDEERS) competition was held thanks to the efforts of the National Applied Research Laboratories (NARLabs), the National Center for Research on Earthquake Engineering (NCREE), and the British Council (BC), on September 18–20, 2015. There were a total of 15 graduate teams, 42 undergraduate teams, and 38 high school teams participating in the IDEERS modeling and testing event this year. The foreign teams came from China, Hong Kong, Indonesia, Japan, Korea, Malaysia, Macao, Philippines, Singapore, and Vietnam.

On September 19, participants had 6.5 hours to complete their models using simple materials and tools including long strips of wood, rectangular wooden base boards, PVC hot melt glues, rubber bands, and string. The theme of this year's competition for high school teams was "asymmetric-plan base". Each high school team had to construct a model that required an asymmetric-plan base designed to resist torsional vibration. The theme of this year's competition for the undergraduate teams was "an elevated first floor". The model that was made by each undergraduate team required the elevated first floor to resist strong ground motions. Every model of the high school teams and undergraduate teams had to resist strong ground motions from 250 cm/sec^2 to 1000 cm/sec^2 while carrying loads of up to 26 kg. Meanwhile, the competition of the postgraduate teams was focused on how to apply advanced technologies to build a seismic structure with energy dissipation and/or seismic isolation. All models were ranked using the efficiency ratio (ER), which was computed based on the mass of the model itself, the number of mass blocks supported by the model, and the PGA eventually resisted by the model. The winner was the team whose model obtained the largest value of ER.



Fig. 1. Models were tested on a shaking table

Participating students showed their creativity with diverse types of structural designs. On September 20, after the opening ceremony, models were tested on a shaking table with earthquakes of different intensities. In the end, the YUNG-NIAN Catholic High School team won first prize in the high school division, the Hong Kong University of Science and Technology team won first prize in the undergraduate division, and the National Taiwan University team won first prize in the graduate division. More information about IDEERS is available at http://www.ncree.org/ideers/2015/.

The International Training Program for Seismic Design of Structures 2015

Chi-Hao Lin, Assistant Researcher, NCREE

Recent major earthquakes around the Pacific Rim and between the Indian and the Eurasian seismic zone have resulted in serious loss of life and damage to property. In order to promote seismic design technology to mitigate seismic hazards in high-seismicity regions such as in South-East Asia and Latin America, the Ministry of Science and Technology (MOST) has continuously sponsored the National Center for Research on Earthquake Engineering (NCREE) to hold the International Training Program for Seismic Design of Structures (ITP). This training program allows participants from the aforementioned areas to learn about earthquake engineering research and practice in Taiwan, to exchange ideas, and share experiences.

The ITP has been held annually since 2002. 413 participants from 23 different countries have attended the training programs from 2002 to 2014. Especially, ITP2015 was a training program of Asia-Pacific Economic Cooperation (APEC). It was held from October 12 to 16, 2015, at the NCREE. A total of 19 technical lectures were scheduled in this program, including topics on seismic observations and hazard analysis; seismic design force; seismic design of structures, bridges, and foundations; seismic evaluation and retrofitting; energy dissipation and isolation systems; seismic loss estimation; and the latest research programs conducted at the NCREE. Fifty-one participants from Guatemala, Indonesia, Jordan, Malaysia, Vietnam, El Salvador, Haiti, Mongolia, Dominican, Philippines and Thailand have successfully completed all of the courses.

In fulfillment of the goals of ITP2015, the seismic design technology and earthquake-resisting capabilities of the participating countries will be steadily improved. We believe that this training program has been successful in strengthening international relationships as well as in sharing experiences on earthquake hazard mitigation.



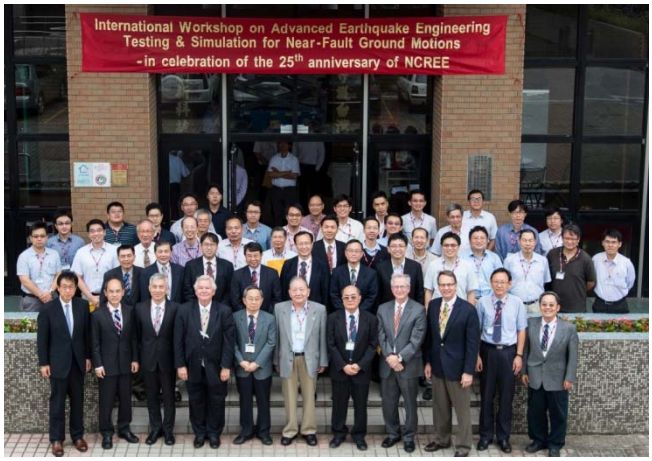
International Workshop on Advanced Earthquake Engineering Testing and Simulation for Near-Fault Ground Motions and Multiple Hazard Load Effects

Task Group for Development of Advanced Experimental Research Initiatives for NCREE Southern Laboratory

The International Workshop on Advanced Earthquake Engineering Testing and Simulation for Near-Fault Ground Motions and Multiple Hazard Load Effects was held on November 19-20, 2015 to celebrate the 25th anniversary of NCREE since its inauguration in 1990. The workshop invited 11 international professors and 8 domestic professors to deliver speeches on advanced earthquake engineering testing and simulation technologies for near-fault ground motions and multiple hazard load effects, and attracted some 110 participants. An electronic copy of the workshop proceedings will be available in early 2016 at the workshop website: http://aeets2015.ncree.org.tw.

In Taiwan, there are twenty Holocene (i.e., Category-I) active faults according to the Central Geological Survey. Based on this fact, 2.5 million buildings and 8.6 million residents live within a 10 km perimeter of these faults. As such, the Ministry of Science and Technology, National Development Council, National Applied Research Laboratories, and National Cheng Kung University (NCKU) jointly support the construction of NCREE Southern Laboratory in the NCKU Kuei-jen (歸仁) Campus to enable research applied to mitigate potential near-fault catastrophic threats. In the immediate neighborhood of the NCREE Southern Laboratory, there are a Fire Experiment Center and a Mock-up Testing and Wind Tunnel Laboratory operated by the Architecture and Building Research Institute (ABRI), the Ministry of Interior. These three labs, when brought together, will be able to form a Research Park for Near-Fault and Multiple Hazards Mitigation. This hazard mitigation Research Park would provide a great opportunity to witness how far academics and professionals can push the boundaries and deal with technological challenges from near-fault threats as well as multiple hazards.

The headquarters laboratory of NCREE in Taipei City houses a 5 m x 5 m triaxial shaking table for real dynamic tests, reaction-wall strong-floor testbed for quasi-static experiments, and a Multi-Axial Testing System (known as MATS) for quasi-static high axial load testing. Over the past years, the NCREE headquarters laboratory has seen its researchers and domestic academics carry out many of the world's cutting edge experiments that created technological breakthroughs in the field of earthquake engineering, and thereby imposed a significant impact on earthquake engineering practice. There have been wonderful moments from utilizing the current facilities, but research is an endless journey. In this regard, the NCREE Southern Laboratory features an 8 m x 8 m high-speed long-stroke triaxial shaking table, and a high speed Bi-Axial Testing System (BATS) for dynamic high axial load testing. The NCREE Southern Laboratory is close to the Taiwan High Speed Rail Station of Tainan and has a comparable floor area to its Taipei Headquarters, but houses far more advanced cutting-edge testing facilities. The NCREE Southern Laboratory is currently under construction and is projected to be completed by the end of 2016, and will be in operation in 2017. The NCREE Southern Laboratory will enable its researchers and domestic academics to boldly explore technological frontiers that have never been visited before.



Goup photo of the workshop speakers and guests

The 5th Taiwan and China Young Scholar's Conference on Earthquake Engineering and the 6th Taiwan BEM Method Conference

Ren-Zuo Wang, Associate Researcher, NCREE

In recent years, earthquakes have occurred frequently in Taiwan and China. They have caused casualties, loss of life, and property damage for the effective to lower people in the earthquake disaster. China's scholars shared new research results and technical exchanges. Thus, the 5th Taiwan and China Young Scholar's Conference on Earthquake engineering and the 6th Taiwan BEM method conference was held from October 18 to 19, 2015 at the NCREE. In Taiwan, this conference was mainly organized by the National Center for Research on Earthquake Engineering (NCREE) of the Republic of China (Taiwan, R.O.C.), National Taiwan University (Department of Civil Engineering), National Taiwan Ocean University (Department of Harbor & River Engineering, NTOU/MSV), China Tsinghua University, Tongji University, Zhejiang University, and Harbin Institute of Technology. The total number of participants was 178. We believe that this conference was successful in sharing experiences on earthquake engineering and numerical simulations.



Fig. 1. Group photo of 5th Taiwan and China Young Scholar's Conference on Earthquake engineering and 6th Taiwan BEM method conference participates

Published by

National Center for Research on Earthquake Engineering

200, Sec. 3, XinHai Rd., Taipei 106, Taiwan, R.O.C.

Phone: 886-2-6630-0888

Fax: 886-2-6630-0858

Website: http://newsletter.ncree.org

The National Center for Research on Earthquake Engineering (NCREE) is a laboratory of National Applied Research Laboratories (NARL)

Website: http://www.narl.org.tw